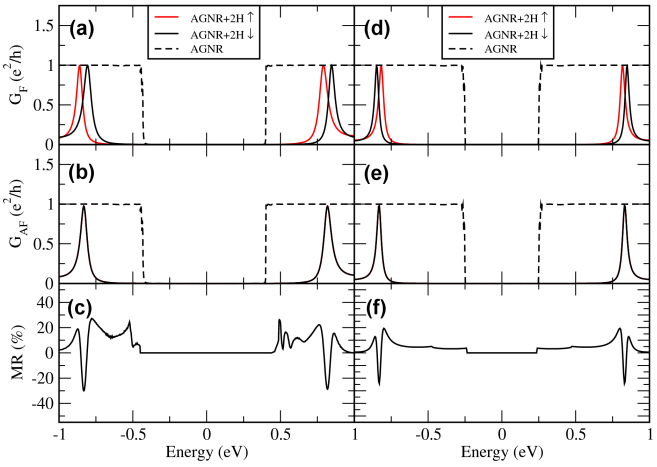

FIG. 5: Spin resolved transmission as a function of energy for the ferromagnetic state of an armchair graphene nanoribbon of width $N = 9$ with two H atoms adsorbed in the middle at a mutual distance $d = 32$ Å calculated in the (a) local spin density approximation and (d) with a one-orbital mean-field Hubbard model. (b) and (e) panels show the same, but for the antiferromagnetic state. The resulting magnetoresistance in both approximations is shown in (c) and (f).

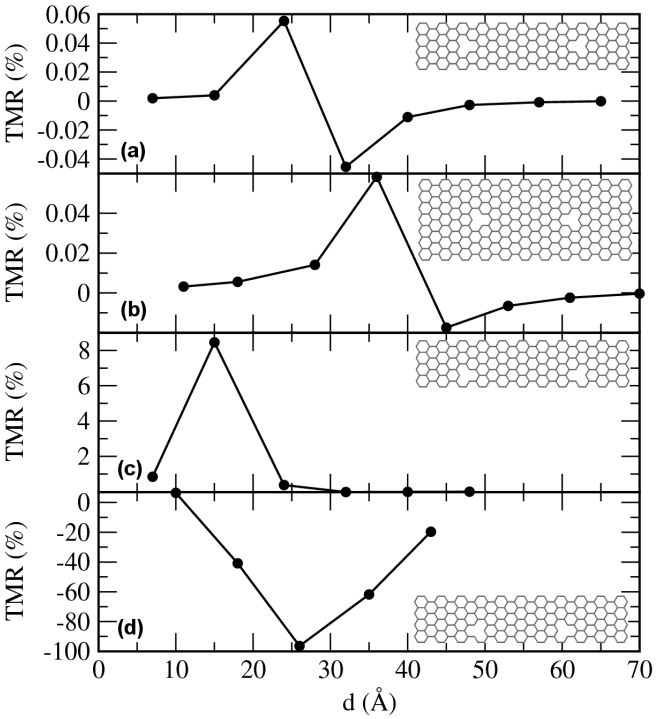

FIG. 6: Tunneling magnetoresistance for four different atomic H configurations. Two H atoms in a head-to-head configuration located in the middle of an armchair graphene nanoribbon of length $L = 73.7$ Å with a width of $N = 9$ (a) and $N = 15$ (b), and two H atoms located near one edge in a head-to-head (c) and in a tail-to-tail (d) configuration for a ribbon width of $N = 9$ and length of $L = 57.0$ Å.

tion, here the electronic structure will be indirectly affected by the field even if its direct influence on the orbital wave function is neglected. This change reflects in the spin-resolved conductance as shown in Fig. 5(a-b) for $d = 32$ Å (the dashed line represents the conductance of the clean AGNR). The different total transmission for the F and AF solutions, resulting from adding the two spin channels, results in a positive magnetoresistance (MR), $MR = G_F - G_{AF}/G_F + G_{AF}$, at energies near the bottom and top of the conduction and valence bands, respectively [see Fig. 5(c)]. Similar results are obtained (not shown) for different intermediate distances between H atoms. The right panels in Fig. 5 show the results obtained from the one-orbital mean-field Hubbard model for $U = t = 3$ eV. Apart from the recovery of the particle-hole symmetry, the results are remarkably similar, validating the use of the latter model for transport calculations in hydrogenated graphene.

One should note, however, that since the chemical potential lies in the middle of the gap, the energy ranges at which MR could manifest itself are not relevant in linear response transport for infinite AGNR's. A finite bias calculation may reveal the MR obtained at those energies, but this is a non-trivial task beyond the scope of this work. The application of a gate voltage is not a practical alternative either since it implies a deviation from charge neutrality which would fill up or empty the localized states hosting the unpaired spins and kill the magnetization. Instead, we propose to explore the possibility of MR at zero bias by considering *finite* AGNR's connected at the ends to conductive graphene. This is done in our calculations by considering a metallic AGNR with a narrower section in the middle of appropriate width [see Fig. 1(d)]. (Note that in the one-orbital mean-field Hubbard approximation AGNR's of width $N = 3m - 1$, where m is an integer, are metallic, being semiconducting otherwise). In what follows and in the light of the previous results, we restrict ourselves to the one-orbital mean-field Hubbard model.

In our proposed AGNR heterostructure the difference in the zero-bias tunnel conductance between the F and AF states is now responsible for the appearance of *tunneling* MR (TMR), as shown in Fig. 6. Notice that unlike conventional TMR, where the magnetic elements are in the electrodes, in our proposal magnetism is in the barrier. Panels (a) and (b) in Fig. 6 correspond to H atoms placed in the middle of a semiconducting AGNR of length $L = 73.7$ Å and width $N = 9$ and $N = 15$, respectively. Both cases refer to head-to-head configurations. The obtained TMR changes sign with d, but it is always negligibly small. On the contrary, when placed near the edge [Fig. 6(c)], the TMR is positive and reaches much larger values. This result is for an $N = 9$, $L = 57.0$ Å AGNR. When the H atoms are now placed in a tail-to-tail configuration near the edge for the same AGNR, the TMR becomes negative and reaches values of up to 100% [see Fig. 6(d)]. As a final example we show in Fig. 7 the TMR for the case where the H atoms are placed